CrossMark

DIAGNOSTIC NEURORADIOLOGY

Frequency and appearance of hemosiderin depositions after aneurysmal subarachnoid hemorrhage treated by endovascular therapy

Bernhard Falter[1] · Martin Wiesmann[1] · Jessica Freiherr[1] · Omid Nikoubashman[1] ·
Michael Mull[1]

Abstract

Introduction It is still unclear how often subarachnoid hemorrhage (SAH) leads to chronic hemosiderin depositions. In this study, we aimed to determine the frequency of chronic hemosiderin depositions after aneurysmal SAH in patients who did not undergo surgery. Furthermore, we analyzed typical MRI patterns of chronic SAH and sought to obtain information on the temporal course of MRI signal changes.

Methods We retrospectively analyzed 90 patients who had undergone endovascular treatment for acute aneurysmal SAH. In all patients, initial CT studies and at least one T2*-weighted MRI obtained 6 months or later after SAH were analyzed for the presence and anatomical distribution of SAH or chronic hemosiderin depositions. In total, 185 T2*-weighted MRI studies obtained between 2 days and 148 months after SAH were evaluated (mean follow-up 30.2 months).

Results On MRI studies obtained later than 6 months after SAH, subpial hemosiderin depositions were found in 50 patients (55.5 %). Most frequent localizations were the parenchyma adjacent to the frontal and parietal sulci and the insular cisterns. While the appearance of hemosiderin depositions was dynamic within the first 3 months, no changes were found during subsequent follow-up. MR signal changes were not only conclusive with subarachnoid hemosiderin depositions but in many cases also resembled those that have been associated with cortical hemosiderosis.

Conclusions T2*-weighted MRI is an effective means of diagnosing prior SAH. Our study suggests that chronic hemosiderin depositions can be found in a considerable number of patients after a single event of subarachnoid hemorrhage.

Introduction

Gradient-echo T2*-weighted MRI has been shown to reliably detect hemosiderin degradation products [1–5]. This method can be used to diagnose both acute and chronic intracranial hemorrhage [5–8]. T2*-weighted imaging has therefore become a routine tool in the diagnosis of, e.g., cerebral cavernomas, amyloid angiopathy, or superficial siderosis.

In patients with intracranial aneurysms, the decision whether to treat the aneurysm or not may depend on knowledge that the aneurysm has ruptured. In some cases, however, subarachnoid hemorrhage (SAH) can be hard to detect. Small hemorrhages can be almost asymptomatic. The sensitivity of CT in the detection of SAH decreases from 85 % in the first day to 50 % after 1 week, and 30 % only after 2 weeks [9]. Cerebrospinal fluid (CSF) examination has a higher sensitivity but will also fail after a few months [10]. It has been shown that hemosiderin depositions (HD) can be detected on T2*-weighted MRI years after an intracranial hemorrhage, possibly even after decades [5, 7]. However, it is still unclear how often SAH leads to chronic HD. To the best of our knowledge, only two studies have looked systematically into the frequency of HD after SAH [11, 12]. Imaizumi et al. found HD in 72.4 % of their patients. However, only patients who had undergone surgical clipping of their aneurysms were included.

✉ Michael Mull
mmull@ukaachen.de

[1] Department of Neuroradiology, University Hospital Aachen RWTH, Pauwelsstr. 30, 52074 Aachen, Germany

Lummel et al., who investigated ruptured aneurysms in 72 patients who underwent endovascular treatment ($n=65$) or surgery ($n=7$), reported HD in 54.2 % of cases after a follow-up of at least 4 months.

In this study, we aimed to determine the dynamic frequency of chronic HD after aneurysmal SAH in patients who received endovascular treatment and who did not undergo surgery. Furthermore, we analyzed typical MRI patterns of chronic SAH and sought to obtain information on the temporal course of MRI signal changes.

Materials and methods

Subjects

After approval by the ethics committee of our university, we retrospectively analyzed all patients admitted to our university hospital between 2000 and 2012 for acute SAH. Patients were included if they fulfilled all the following criteria: (a) CT available on admission or the following day, (b) proven aneurysms likely the cause of SAH using digital subtraction angiography, (c) SAH proven by CT or lumbar puncture, (d) aneurysm treatment by endovascular therapy, and (e) at least one MRI with T2* imaging 6 months or later after the SAH. Exclusion criteria were any surgical aneurysm clipping or surgical trepanation within 6 months after the SAH. If patients underwent secondary surgical treatment later than 6 months, only the MRI examinations before surgery were analyzed. In total, 90 patients fulfilled all the above criteria.

For each patient, the following data were noted: age, gender, dates of SAH and imaging studies, severity of SAH as documented by the World Federation of Neurosurgical Societies (WFNS) score on admission [13], severity of SAH as documented by the Fisher score [14], presence of intraventricular hemorrhage, and treatment by external ventricular drainage or ventricular shunt.

Neuroradiological studies

First, if patients underwent more than one cranial CT examination in the first week after SAH, we selected the study which demonstrated the largest extent of subarachnoid hemorrhage. This was done in order not to underestimate the extent of a hemorrhage if an early rebleed occurred. Next, we selected all MRI studies before or after 6 months after SAH which contained T2*-weighted gradient-echo images.

MRI and CT scans of each patient were viewed together to, e.g., discern between calcifications and HD of the falx cerebri. Two readers, of whom one was a neuroradiologist with more than 10 years of clinical experience, performed evaluations as consensus readings. In 79 patients (87 %), MRI studies were performed on a 1.5-T MRI scanner only (Philips Gyroscan).

In nine patients (10 %), MRI studies were performed on both a 1.5-T and a 3-T MRI scanner (Philips Achieva 3T). In two patients (3 %), the MRI studies were performed on the 3-T MRI only.

From the selected MRI studies, only the T2*-weighted gradient-echo images were analyzed systematically in the context of this study. Typical sequence parameters at 1.5 T (3 T) were repetition time 658 ms (707 ms), echo time 14 ms (16 ms), flip angle 18° (18°), matrix 256×256 (256×256), field of view 230 mm (230 mm), and slice thickness 4 mm (5 mm). HD that had developed from hematomas were observed as focal areas of signal loss (linear, curvilinear, and spotty low intensity). Corresponding CT images were compared to rule out cerebral calcifications. From the MRI studies, fluid-attenuated inversion recovery (FLAIR), T1-weighted (T1w) and T2w images, and time-of-flight (TOF) MR angiography images were compared to discern HD from cerebral arterial and venous flow voids.

To characterize typical MRI patterns of chronic SAH on T2*-weighted images, we noted whether the areas of signal loss resembled "clots" (focal hypointensities in sulci or ventricles), were "linear superficial" (thin linear hypointensities along the pia mater in the sulci or basal cisterns), or were "linear superficial with tram-track sign" (two thin linear hypointensities along the pia mater of corresponding faces of the sulci or basal cisterns).

Distribution of hyperdense subarachnoid blood on initial CT scans and hypointense HD on T2*-weighted images was noted separately for 33 anatomical regions (as detailed in Table 1). Parenchymal hematomas were noted separately.

Temporal evolution of hemosiderin depositions

In all patients who underwent multiple MRI examinations, we consecutively compared the MRI studies to obtain information on the temporal evolution of HD. We separately analyzed temporal dynamics between the first 8 weeks after the SAH and all images obtained later than 3 months (period 1), between 2 and 4 months after SAH and all images obtained later than 6 months (period 2), and between 5 and 7 months after SAH and all images obtained later than 9 months (period 3).

Statistical analysis

The Student t test was used for the variable age; the Mann-Whitney U test was used to compare the variables WFNS score and Fisher classification; the chi-squared test was used to compare the variable gender, external ventricular drainage, permanent ventricular shunt, and intraventricular hemorrhage. P values <0.05 were considered significant.

Table 1 Detailed localization of blood on initial cranial CT studies and hemosiderin depositions on T2*-weighted MRI studies obtained later than 6 months after subarachnoid hemorrhage in 90 patients

	CT (n=90)	MRI (n=90)
Frontal interhemispheric fissure	54 (60.0 %)	15 (16.7 %)
Dorsal interhemispheric fissure	10 (11.1 %)	5 (5.6 %)
Tentorium	27 (30.0 %)	15 (16.7 %)
Callosal cistern	9 (10.0 %)	1 (1.1 %)
Right sylvian cistern	72 (80.0 %)	8 (8.9 %)
Left sylvian cistern	70 (77.8 %)	8 (8.9 %)
Right insular cistern	59 (65.6 %)	17 (18.9 %)
Left insular cistern	55 (61.1 %)	19 (21.1 %)
Suprasellar cistern	47 (52.2 %)	0 (0.0 %)
Right mesencephalic cistern	60 (66.7 %)	4 (4.4 %)
Left mesencephalic cistern	56 (62.2 %)	8 (8.9 %)
Prepontine cistern	56 (62.2 %)	4 (4.4 %)
Medullary cistern	29 (32.2 %)	4 (4.4 %)
Right cerebellopontine angle cistern	8 (8.9 %)	0 (0.0 %)
Left cerebellopontine angle cistern	11 (12.2 %)	0 (0.0 %)
Superior cerebellar cistern	12 (13.3 %)	8 (8.9 %)
Interpeduncular cistern	60 (66.7 %)	9 (10.0 %)
Right cerebellar sulci	10 (11.1 %)	3 (3.3 %)
Left cerebellar sulci	12 (13.3 %)	3 (3.3 %)
Right lateral ventricle	47 (52.2 %)	8 (8.9 %)
Left lateral ventricle	49 (54.4 %)	7 (7.8 %)
Third ventricle	33 (36.7 %)	1 (1.1 %)
Fourth ventricle	39 (43.3 %)	1 (1.1 %)
Right central sulcus	6 (6.7 %)	4 (4.4 %)
Left central sulcus	6 (6.7 %)	6 (6.7 %)
Right frontal sulci	26 (28.9 %)	23 (25.6 %)
Left frontal sulci	16 (17.8 %)	22 (24.4 %)
Right parietal sulci	14 (15.5 %)	23 (25.6 %)
Left parietal sulci	13 (14.4 %)	20 (22.2 %)
Right occipital sulci	4 (4.4 %)	4 (4.4 %)
Left occipital sulci	3 (3.3 %)	2 (2.2 %)
Right temporal sulci	8 (8.9 %)	10 (11.1 %)
Left temporal sulci	6 (6.7 %)	7 (7.8 %)

CSF localizations refer to subpial surfaces adjacent to the respective CSF spaces

Results

Patient demographics and clinical data

Of the 90 patients, 16 (18.0 %) were male and 74 (82.0 %) were female. On average, patients were 51 years old (standard deviation 13.5, range 21–80 years). The average WFNS score on admission was 2.85 (SD 1.2, range 1–5). Hunt and Hess distribution was as follows: I 9 (10 %), II 33 (36 %), III 24 (27 %), IV 11 (12 %), and V 13 (14 %). The average Fisher score was 2.91 (SD 0.66, range 1–4). In 62 of the 90 patients

(68.9 %), intraventricular hemorrhage was detected. In 33 patients (36.7 %), a temporary external ventricular drainage was placed. Seventeen patients (18.9 %) received a permanent ventricular shunt. To the best of our knowledge, none of the patients had a history of a previous SAH. According to medical reports, three patients suffered from epilepsy during follow-up; there was gliosis of the temporal lobe in two of these patients. No patient suffered from hearing loss or progressive dementia.

MRI studies

In total, 185 MRI studies fulfilled our criteria. In 28 patients, only one MRI study was available. In 31 patients, two MRI studies were available. In 29 patients, three MRI studies were available. In two patients, four MRI studies were available. MRI studies were performed between 2 days and 148 months after SAH. In total, 36 MRI studies were performed in the first month after SAH; 48 studies were performed between 2 and 5 months after SAH; and 137 studies were performed later than 6 months after SAH. Mean follow-up time was 30.2± 28.4 months (median 21.5; 6–147). In the nine patients, who underwent imaging at both 1.5 and 3 T, intraindividual frequency and distribution of hemosiderin depositions was comparable and did not depend on field strength.

Frequency and distribution of hemosiderin depositions

When only MRI studies obtained later than 6 months after SAH were evaluated, 33 patients (36.7 %) showed no evidence of subarachnoid hemorrhage on T2*-weighted MRI (Fig. 1). Overall, hemosiderin was found in 57 patients (63.3 %). In 50 patients (55.5 %), hemosiderin was found in the subpial parenchyma (Fig. 2). There were isolated intraventricular and (sub)dural HD in one and two patients, respectively (3.3 %). Isolated parenchymal HD was found in four patients (4.4 %). Parenchymal HD were caused either by the
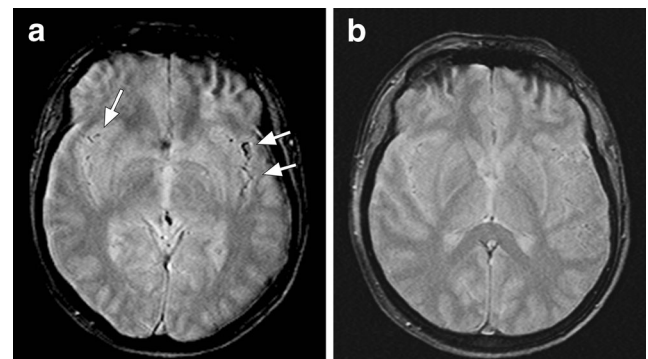
Fig. 1 T2*-weighted gradient-echo MRI in a 56-year-old patient suffering from aneurysmal SAH. First MRI 12 days after SAH (**a**) shows blood residues in the sylvian and insular cistern on both sides (*arrows*). Six months later (**b**), the blood residues were absorbed
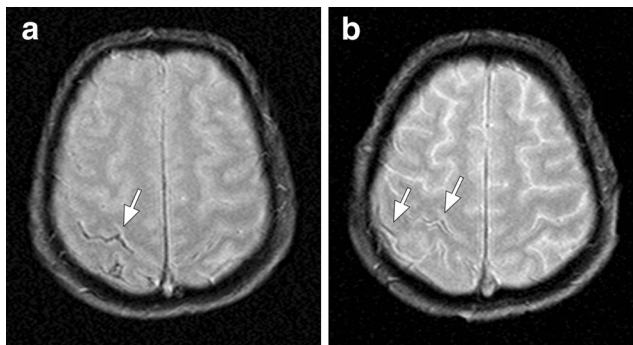
Fig. 2 T2*-weighted gradient-echo MRI in a 58-year-old patient suffering from aneurysmal SAH. First MRI 22 days after SAH (**a**) shows blood residues in the central sulcus and parietal sulci on the right side (*arrow*). Nearly 1 year later (**b**), hemosiderin can still be observed in the central sulcus and in parietal sulci on the right side (**b**; *arrows*). Hemosiderin depositions appear as hypointense lines

primary SAH, by secondary hemorrhagic infarction, or as a consequence of ventricular drainage.

The distribution of blood on initial cranial CT studies and HD on T2*-weighted images of MRI studies obtained later than 6 months after SAH is detailed in Table 1. On initial CT, the CSF spaces most frequently affected were the sylvian cisterns, insular cisterns, and the interpeduncular cistern. In contrast to this, on MRI later than 6 months after SAH, the CSF spaces, respectively the adjacent subpial parenchyma, most frequently affected comprised frontal and parietal sulci and the insular cisterns. Subpial HD after 6 months were found adjacent to supratentorial sulci in 42 patients (84 %), adjacent to infratentorial cisterns in 35 patients (70 %).

Temporal dynamics of blood degradation products

Period 1: Thirty-five patients fulfilled the required criteria: MRI scans were available both within the first 8 weeks after SAH and later than 3 months after SAH, and blood degradation products were noted on MRI scans. Five out of 35 patients had unchanged blood degradation products in this period (14.3 %), 28 had a decrease in unchanged localization (82.4 %), and one patient had new blood degradation products in a new localization, but overall a decrease of blood degradation products (2.9 %). Mean follow-up period was 17 ± 8.7 months (median 15; 6–84).

Period 2: Three patients fulfilled the required criteria: MRI scans were available both within 2 to 4 months after SAH and later than 6 months after SAH, and blood degradation products were noted on MRI scans. All three patients showed unchanged blood degradation depositions during this period (100 %). Mean follow-up period was 33 ± 44.2 months (median 44; 6–84).

Period 3: Thirteen patients fulfilled the required criteria: MRI scans were available both within 4 to 7 months after SAH and later than 9 months after SAH, and blood degradation products were noted on MRI scans. All 13 patients showed unchanged blood degradation depositions during this period (100 %). Mean follow-up period was 24.3 ± 21.6 months (median 18; 9–84).

**Hemosiderin depositions after parenchymal bleeding**

Parenchymal hemorrhages were observed in 21 of 90 patients. Follow-up MRI images obtained later than 6 months showed HD in the location of the initial hemorrhage in all 21 patients (100 %).

Imaging characteristics of chronic hemosiderin depositions

A tram-track sign was observed in 34 of 50 (68 %) cases with subpial HD (Fig. 3). Imaging characteristics of chronic HD are detailed in Table 2. It was noted that the linear subpial HD in our cases resembled the linear superficial cortical hemosiderosis which has been reported in patients with cerebral amyloid angiopathy [15].

Permanent ventricular shunt and its impact on later hemosiderin depositions

In 73 of our 90 patients, no permanent ventricular shunt was implanted. In 40 of these 73 patients, HD were noted on MRI scans (54.8 %), while in 33 of these 73 patients, no HD were noted (45.2 %). Seventeen of our 90 patients received a permanent ventricular shunt. All these 17 patients showed permanent HD on MRI scans (100 %) (Fig. 4).
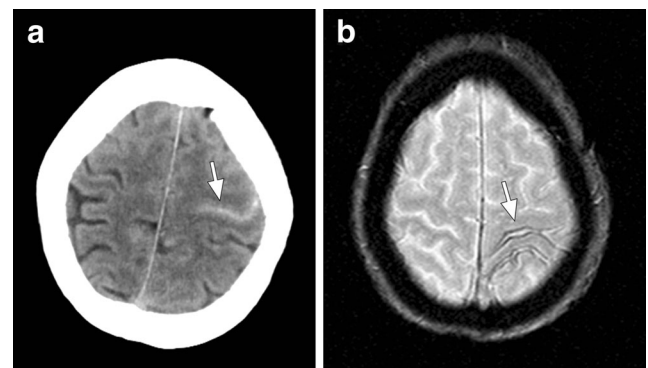
Fig. 3 CT on admission (**a**) and T2*-weighted gradient-echo MRI after 1 year (**b**) in a 78-year-old patient suffering from aneurysmal SAH. CT on admission shows blood in the central sulcus on the left side (*arrow*). One year later (**b**), hemosiderin can be seen in the central (*arrow*) and postcentral sulcus on the *left side*. Note that signal in the affected sulci is hyperintense whereas both surfaces of the adjacent cortices show thin linear hypointensities (tram-track sign). This is characteristic of cortical hemosiderosis

Table 2 Detailed imaging characteristics of chronic hemosiderin depositions on T2*-weighted MRI studies obtained later than 6 months after subarachnoid hemorrhage in 51 patients

	n (%)
Intraventricular hemosiderin clots only	1 (2 %)
Linear superficial hemosiderin depositions (without tram-track sign)	13 (25 %)
Sulcal hemosiderin clots and linear superficial hemosiderin depositions (without tram-track sign)	3 (6 %)
Linear superficial hemosiderin depositions with tram-track sign	31 (61 %)
Sulcal hemosiderin clots and linear superficial hemosiderin depositions with tram-track sign	3 (6 %)

Six patients with isolated parenchymal or (sub)dural hemosiderin depositions were excluded

Statistical analysis

In the univariate analysis, the following features were significantly correlated with the appearance of HD: ventricular drainage, permanent ventriculoperitoneal shunt, intraventricular hemorrhage, WFNS score, and Fisher score (Table 3).

Discussion

It is assumed that subarachnoid hemosiderin depositions are usually the result of repetitive subarachnoid hemorrhage [16]. The term superficial siderosis is used for this entity, with vascular malformations, hemorrhagic tumors, or cerebral amyloid angiopathy among the most frequent causes [17]. Furthermore, it has recently been reported that traumatic SAH and chronic subdural hematoma can lead to superficial siderosis [18, 19].

Imaizumi et al. also identified subarachnoid hemorrhage due to aneurysm bleeding as a cause for HD. They studied 58 patients between 3 and 18 months after aneurysmal SAH

Fig. 4 T2*-weighted gradient-echo MRI in a 49-year-old patient obtained 4 years after aneurysmal SAH. Chronic hemosiderin depositions are observed as superficial linear hypointensities in multiple cortical sulci (*white arrows*). There is also a focal parenchymal hemosiderin deposit (*black arrow*) after surgical treatment (ventricular catheter)

and reported HD in 72.6 % of their patients [11]. However, they included only patients undergoing surgical therapy, consequently making the distinction between aneurysmal and iatrogenic HD difficult. Inoue et al. studied 50 patients suffering from aneurysmal SAH and found subarachnoid hypointensities on T2*-weighted images in all patients [5]. However, MRI examinations were performed between the day of hemorrhage and as late as 16 years after hemorrhage. Only 15 patients were studied later than 6 months after SAH. Interestingly, this study shows that subarachnoid HD can persist as long as 16 years after SAH. Takada et al. studied 49 patients before they underwent open surgery of an intracranial aneurysm with no history of a subarachnoid hemorrhage [2]. In nine patients, HD were noted during surgery. In four of those patients, the HD had also been observed on T2*-weighted MRI. The authors concluded that T2*-weighted MRI may have the potential to detect clinically silent minor hemorrhages from an aneurysm. Recently, Lummel et al. reported 39 cases of HD in 72 patients (54.2 %) with a follow-up of at least 4 months after subarachnoid hemorrhage [12]. We found a highly comparable frequency of 55.5 % (50/90) of patients with subpial HD. With regard to the low frequency of 8 % in presumably non-hemorrhagic aneurysms reported be Takada et al., our data suggest that a single event of subarachnoid hemorrhage can also lead to chronic subarachnoid HD and that their frequency is much higher than previously assumed. Of course, it is possible that a single clinical event of SAH was preceded by multiple small occult SAH, but it is unlikely that this was the case in the majority of our patients. Even though the available data do not yet allow defining the true frequency of chronic HD after aneurysmal SAH, it seems reasonable to expect that chronic HD can be found in the majority of patients.

Our study presents evidence that the anatomical distribution of subarachnoid blood and its remnants change during the first months and then remain stable in long-term follow-up. More specifically, we found that while the appearance of HD changed during the first 3 months, the appearance of HD in all 15 patients with the first follow-up imaging after at least 2 months and the second follow-up imaging after at least 6 months remained unchanged during a mean observation period of 22.1+20.8 months (median 12, 6–84). On initial CT, the CSF spaces most frequently affected were the sylvian cisterns, the insular cisterns, and the interpeduncular cistern. This corresponds well with the site of aneurysm rupture and initial distribution of hemorrhage. On MRI images obtained later than 6 months after SAH, the sites most frequently affected comprised frontal and parietal sulci and the insular cisterns, but also along the interhemispheric fissures or the tentorium. This may be due to turbulent CSF flow which can wash away blood clots in areas like the basal cisterns but may also lead to redistribution of blood products and formation of HD in areas distant to the site of aneurysm rupture.

Table 3 Univariate analysis of features with possible correlation to the appearance of chronic hemosiderin depositions after subarachnoid hemorrhage

Univariate analysis	With hemosiderin[a]	Without hemosiderin[a]	P value	Type of test
Number	57	33		
Sex (female)	48/9	26/7	0.5732	X^2 (chi-square)
Ventricular drainage	31/26	2/31	<0.0001	X^2 (chi-square)
Permanent ventricular shunt	17/40	0/33	<0.0001	X^2 (chi-square)
Intraventricular hemorrhage	47/10	15/18	0.0003	X^2 (chi-square)
WFNS score	3.18±1.21	2.30±0.98	0.0008	Mann-Whitney U
Fisher score	3.11±0.59	2.58±0.66	0.0004	Mann-Whitney U
Age	52.93±13.14	48.39±12.55	0.1089	Student's T

[a] Coding of the categories of two variables by means of 0 and 1. 1 is the affirmative component, and 0 is the negative component. Example hemosiderin/permanent ventricular shunt: 17 patients received a permanent ventricular shunt and 40 patients received no permanent ventricular shunt

Imaizumi et al. also reported that HD were often found in parietal sulci distant from ruptured aneurysms [11].

In our study, factors statistically associated with the development of chronic HD after SAH included placement of ventricular drainage, implantation of a permanent ventriculoperitoneal shunt, presence of intraventricular hemorrhage, and higher scores on the WFNS score, as well as on the Fisher score (Table 3). All these factors are indicative of the severity of the initial subarachnoid hemorrhage. Any clinical study including patients treated for symptomatic aneurysmal SAH, such as ours, will predominantly consist of patients suffering from moderate to severe SAH. This selection bias needs to be considered. So far, no data are available to conclude how often chronic HD may be observed after minor aneurysmal SAH or non-aneurysmal perimesencephalic SAH.

Imaizumi et al. suggested that surgical therapy should reduce the frequency of chronic subarachnoid HD after aneurysmal SAH [11]. They hypothesized that the washout of subarachnoid hematoma fluid during a surgical operation as well as postoperative CSF drainage (cisternal and ventricular drainages) would accelerate the clearance of blood from the subarachnoid space and thus reduce the extent of hemosiderin deposition. Our data do not support this hypothesis. We found HD in 55.5 % of our patients, who all underwent endovascular treatment, whereas Imaizumi et al. reported HD in 72.6 % of their patients, who all underwent surgical therapy.

Although the number of patients studied is too small to allow definitive conclusions, our results are indicative of two findings: (a) The extent of subarachnoid hypointensities on T2*-weighted images observed within 8 weeks after SAH usually decreases over time. In our series, this was observed in 85.3 % of cases. Pathophysiologically, these hypointensities correspond to deoxyhemoglobin and methemoglobin in subarachnoid blood clots, which are diluted and washed away by CSF over time; (b) hypointensities on T2*-weighted images, which are noted 6 months or later after SAH, remain unchanged over time. In our series, this was true in all cases. Pathophysiologically, this corresponds to chronic HD on

subarachnoid membranes or in the subpial layer [15]. Our results are in line with the findings of Takada et al., who suggested that from 3 months after SAH, hypointensities on T2*-weighted images may remain constant [2]. It should be noted, however, that in their series, only five patients were studied later than 3 months after SAH.

Recently, it has been reported that subarachnoid hemosiderosis and superficial cortical hemosiderosis are signs of cerebral amyloid angiopathy [15, 20]. It is assumed that repeated minor subarachnoid bleeds from small arterial and venous vessels affected by amyloid angiopathies lead to chronic HD and that hemosiderin on subarachnoid membranes can be taken up into subpial cortical layers. On T2*-weighted images, superficial cortical hemosiderosis is typically characterized by thin hypointense lines on both cortical surfaces adjacent to a cortical sulcus which shows hyperintense signal ("tram-track sign"). This sign has been reported to be highly specific for amyloid angiopathy [15]. It is a significant finding of our study that in most cases, the typical imaging characteristics of superficial cortical hemosiderosis can also be observed in the chronic phase after single aneurysmal SAH. In our series, we observed single linear superficial HD in 50 of 90 cases (55.5 %) and the tram-track sign in 34 of 90 cases (37.8 %). To the best of our knowledge, this has not been reported before.

Limitations

The present study has several limitations: (a) We did not perform sequential MRI studies in all patients. Consequently, a prospective serial study is needed to further define the temporal course of blood degradation products after SAH. (b) Our study is biased toward patients with moderate to severe SAH. Additional studies should also include patients with minor aneurysmal SAH and non-aneurysmal perimesencephalic SAH. (c) Only anecdotal observations are available on the persistence of chronic HD after years. Long-term follow-up

examinations are therefore required. (d) Recently, susceptibility-weighted imaging (SWI) MR sequences have been introduced. This technique offers a higher geometric resolution than T2*-weighted gradient-echo sequences but is also very sensitive to susceptibility artifacts [21, 22]. Using SWI sequences may increase the sensitivity for detection of chronic HD after SAH. Signal loss on gradient-echo T2*-weighted MR images is characteristic of hemoglobin degradation products both in the acute, subacute, and chronic phase [8]. Acute SAH often affects the basal cisterns. In this location, T2*-weighted gradient-echo images may be impaired by susceptibility artifacts caused by air/bone interfaces. In the literature, FLAIR or proton-density-weighted spin-echo sequences have therefore been recommended to detect acute SAH [23–27]. This technique is based on the fact that any subarachnoid hemorrhage increases the protein concentration in CSF. Increased protein concentration can be detected after SAH for weeks although data on this are scarce. In contrast, T2*-weighted MRI is superior to detect chronic HD and has been reported as late as 20 years after hemorrhage [5, 28]. However, signal loss on gradient-echo T2*-weighted MRI is unspecific and can also represent calcification, physiological ferritin, melanoma, air, and some paramagnetic contrast agents. Accordingly, in this study, we compared T2*-weighted images with corresponding CT images to rule out cerebral calcifications, as well as with FLAIR, T1w and T2w images, and time-of-flight (TOF) MR angiography images to discern HD from cerebral arterial and venous flow voids.

References

1. Gomori JM, Grossman RI, Hackney DB, Goldberg HI, Zimmerman RA, Bilaniuk LT (1988) Variable appearances of subacute intracranial hematomas on high-field spin-echo MR. AJR Am J Roentgenol 150(1):171–178
2. Takada S, Inoue T, Niizuma K, Shimizu H, Tominaga T (2011) Hemosiderin detected by T2*-weighted magnetic resonance imaging in patients with unruptured cerebral aneurysms: indication of previous bleeding? Neurol Med Chir (Tokyo) 51(4):275–281
3. Horita Y, Imaizumi T, Hashimoto Y, Niwa J (2008) Subarachnoid hemosiderin deposition after subarachnoid hemorrhage on T2*-weighted MRI correlates with the location of disturbed cerebrospinal fluid flow on computed tomography cisternography. Neurol India 56(1):62–64
4. Toyama K, Imaizumi T, Yoshifuji K, Miyata K, Kawamura M, Kohama I (2005) Study on hemosiderin deposition after intracerebral hemorrhage. No Shinkei Geka 33(12):1177–1181
5. Inoue T, Takada S, Shimizu H et al (2013) Signal changes on T2*-weighted magnetic resonance imaging from the acute to chronic phases in patients with subarachnoid hemorrhage. Cerebrovasc Dis 36(5-6):421–429
6. Kinoshita T, Okudera T, Tamura H, Ogawa T, Hatazawa J (2000) Assessment of lacunar hemorrhage associated with hypertensive stroke by echo-planar gradient-echo T2*-weighted MRI. Stroke 31(7):1646–1650
7. Yuan MK, Lai PH, Chen JY et al (2005) Detection of subarachnoid hemorrhage at acute and subacute/chronic stages: comparison of four magnetic resonance imaging pulse sequences and computed tomography. J Chin Med Assoc 68(3):131–137
8. Wiesmann M, Mayer TE, Yousry I, Hamann GF, Brückmann H (2001) Detection of hyperacute parenchymal hemorrhage of the brain using echo-planar T2*-weighted and diffusion-weighted MRI. Eur Radiol 11(5):849–853
9. van Gijn J, van Dongen KJ (1982) The time course of aneurysmal haemorrhage on computed tomograms. Neuroradiology 23(3):153–156
10. Ito U, Inaba Y (1973) Cerebrospinal fluid cytology for detection of subarachnoid hemorrhage long after the attack and estimation of post-hemorrhagic duration. Rinsho Shinkeigaku 13(5):283–290
11. Imaizumi T, Chiba M, Honma T, Niwa J (2003) Detection of hemosiderin deposition by T2*-weighted MRI after subarachnoid hemorrhage. Stroke 34(7):1693–1698
12. Lummel N, Bernau C, Thon N, Bochmann K, Linn J (2015) Prevalence of superficial siderosis following singular, acute aneurysmal subarachnoid hemorrhage. Neuroradiology 57(4):349–356. doi:10.1007/s00234-014-1480-6
13. Teasdale GM, Drake CG, Hunt W, Kassell N, Sano K, Pertuiset B, De Villiers JC (1988) A universal subarachnoid hemorrhage scale: report of a committee of the World Federation of Neurosurgical Societies. J Neurol Neurosurg Psychiatry 51(11):1457
14. Fisher CM, Kistler JP, Davis JM (1980) Relation of cerebral vasospasm to subarachnoid hemorrhage. Neurosurgery 6(1):1–9
15. Linn J, Herms J, Dichgans M, Brückmann H, Fesl G, Freilinger T, Wiesmann M (2008) Subarachnoid hemosiderosis and superficial cortical hemosiderosis in cerebral amyloid angiopathy. AJNR Am J Neuroradiol 29(1):184–186
16. Kumar N (2010) Neuroimaging in superficial siderosis: an in-depth look. AJNR Am J Neuroradiol 31(1):5–14
17. Spitzer C, Mull M, Rohde V, Kosinski CM (2005) Non-traumatic cortical subarachnoid haemorrhage: diagnostic work-up and aetiological background. Neuroradiology 47:525–531
18. Kakeda S, Korogi Y, Ohnari N, Nishimura J, Moriya J et al (2010) Superficial siderosis associated with a chronic subdural hematoma: T2-weighted MR imaging at 3T. Acad Radiol 17:871–876. doi:10.1016/j.acra.2010.02.014
19. Zhao H, Wang J, Lu Z, Wu Q, Lv H, Liu H, Gong X (2015) Superficial siderosis of the central nervous system induced by a single-episode of traumatic subarachnoid hemorrhage: a study using MRI-enhanced gradient echo T2 star-weighted angiography. PLoS One 10(2):e0116632
20. Lummel N, Wollenweber FA, Demaerel P, Bochmann K, Malik R, Opherk C, Linn J (2015) Clinical spectrum, underlying etiologies and radiological characteristics of cortical superficial siderosis. J Neurol
21. Guo LF, Wang G, Zhu XY, Liu C, Cui L (2013) Comparison of ESWAN, SWI-SPGR, and 2D T2*-weighted GRE sequence for depicting cerebral microbleeds. Clin Neuroradiol 23(2):121–127
22. Yilmaz U, Körner H, Meyer S, Reith W (2014) Multifocal signal loss at bridging veins on susceptibility-weighted imaging in abusive head trauma. Clin Neuroradiol

23. Noguchi K, Ogawa T, Inugami A, Toyoshima H, Okudera T, Uemura K (1994) MR of acute subarachnoid hemorrhage: a preliminary report of fluid-attenuated inversion-recovery pulse sequences. AJNR Am J Neuroradiol 15(10):1940–1943

24. Noguchi K, Ogawa T, Seto H et al (1997) Subacute and chronic subarachnoid hemorrhage: diagnosis with fluid-attenuated inversion-recovery MR imaging. Radiology 203(1):257–262

25. Wiesmann M, Mayer TE, Medele R, Bruckmann H (1999) Diagnosis of acute subarachnoid hemorrhage at 1.5 Tesla using proton-density weighted FSE and MRI sequences. Radiologe 39(10):860–865

26. Wiesmann M, Mayer TE, Yousry I, Medele R, Hamann GF, Bruckmann H (2002) Detection of hyperacute subarachnoid hemorrhage of the brain by using magnetic resonance imaging. J Neurosurg 96(4):684–689

27. Lummel N, Wiesmann M, Brückmann H, Linn J (2010) The value of different magnetic resonance imaging sequences for the detection of intraventricular hemorrhages. Clin Neuroradiol 20(1):38–47

28. McCarron MO, McKinstry CS, Gibson JM (2002) Superficial siderosis 20 years after brain tumour. Lancet Neurol 1(5):326